



# OPEN Comparing the efficacy and safety of cryoablation and microwave ablation in treating paravertebral metastases of rabbit VX2 tumor

Zhenzhen Song<sup>1,2</sup>, Yanfen Zhao<sup>1</sup>, Zhu Liu<sup>1</sup> & Bing Li<sup>1</sup>✉

We sought to assess and compare the effectiveness and safety of cryoablation (CA) and microwave ablation (MWA) in treating paravertebral metastases of VX2 in rabbits. A rabbit VX2 paravertebral metastases model was established under computed tomography (CT) guidance, with a modeling success rate of 88.23% (60/68). Sixty successfully modeled rabbits were randomly allocated into the MWA group ( $n=30$ ) and CA group ( $n=30$ ). A comparative analysis between the CA and MWA groups included assessments of the complete ablation rate, operation time, post-ablation pain, and complication rate. The complete ablation rate in the CA group (86.67%) was higher than that in the MWA group (63.33%) ( $P<0.05$ ), and the operation time in the CA group was notably longer than that in the MWA group ( $P<0.05$ ). The BRPS (Bristol Rabbit Pain Scale) scores in both groups decreased at 5 time points after treatment, the post-treatment points scores in the CA group were lower than those in the MWA group ( $P<0.001$ ). At a follow-up of 21 days postoperatively, the complication rate in the CA group (10.00%) was significantly lower than that in the MWA group (33.33%) ( $P<0.05$ ), with 6 rabbits in the MWA group experiencing severe complications. Compared to MWA, CA for paravertebral metastases demonstrates higher efficacy and safety.

## Abbreviations

CT	Computer tomography
MR	Magnetic resonance
CA	Cryoablation
MWA	Microwave ablation
BRPS	Bristol rabbit pain scale

In recent years, the incidence of malignant tumors has witnessed a notable increase, and a majority of advanced malignant tumors tend to metastasize. When metastatic tumors are situated in the paravertebral region, they frequently induce severe pain and motor dysfunction in patients<sup>1,2</sup>. Paravertebral metastatic tumors, due to their unique anatomical location, involve the paravertebral bone cortex, periosteum, and surrounding soft tissues, which harbor a greater density of sensory nerve endings. Tumor infiltration into muscles and nerves can trigger reactive muscle spasms, often leading to intense and refractory pain. Concurrently, as the tumor progresses, it may precipitate pathological fractures and spinal stenosis, culminating in movement disorders or even paralysis, significantly compromising the patient's overall quality of life<sup>3,4</sup>.

Ablation techniques have emerged as crucial modalities in tumor therapy. Cryoablation (CA) and microwave ablation (MWA), widely applied in clinical interventions for treating tumors in organs like the liver, lungs, and soft tissues, have demonstrated efficacy<sup>5,6</sup>. The theoretical advantage of MWA lies in its ability to generate higher temperatures more quickly and uniformly, offering better control over tissue necrosis; however, the ablation zone is difficult to control precisely. Given the proximity of paravertebral tumors to the dural sacs and nerve roots, there is a potential risk for spinal cord and nerve damage to occur during ablation therapy, leading to severe complications like lower-limb dysfunction. An ice ball generated by CA can be clearly visualized under imaging guidance, which helps control the ablation zone and theoretically reduces the risk of spinal cord and nerve damage. But notably, comparative studies on the short-term efficacy and safety of CA and MWA in treating paravertebral metastatic tumors are lacking. Therefore, the present study aims to establish a rabbit model of

<sup>1</sup>Department of Radiology, Affiliated Hospital of North Sichuan Medical College, 63 Wenhua Road, Nanchong City 637000, Sichuan Province, People's Republic of China. <sup>2</sup>Department of Radiology, No.971 Hospital of Navy, 6 Shandong Road, Qingdao 266000, Shandong, People's Republic of China. ✉email: cbylb@qq.com

paravertebral metastatic tumors and systematically compare the efficacy and safety of the two ablative methods. The findings of this investigation may provide a foundation for guiding clinical interventions in paravertebral metastatic tumors.

Materials and methods

Animals

Sixty-eight healthy large New Zealand White rabbits, all males, with a weight range of 2.5–3.5 kg and an age of 4–6 months, were enrolled in the study. Each rabbit possessed health quarantine certificates. The Animal Ethics Committee of North Sichuan Medical College granted approval for the experimental study (approval no. NSMC Ethical Animal Review (2023)067). This study is in accordance with ARRIVE guidelines. Additionally, two male VX2 tumor-bearing rabbits weighing 2.5 and 2.6 kg were supplied by Hangzhou Huashu Biotechnology Co., China.

Experimental equipment

Scanning equipment included a 3.0-T magnetic resonance (MR) scanner (Area; Siemens, Munich, Germany) with a coil for animal experiments, with specific MR scanning parameters (Table 1) as well as a 16-row spiral CT scanner (Philips Healthcare Ltd., Eindhoven, the Netherlands), with CT scanning parameters of a layer thickness of 2.0 mm, window width of 250 HU, and window position of 35 HU. Ablation equipment included a cryotherapy instrument from Shanghai Orientation Medical Systems (AT-2008-1; CryoHit argon-helium CA system) and a microwave multifunctional treatment instrument from Jiangsu Kangyou Medical Equipment Co. (KY-2000).

CT-guided rabbit VX2 paravertebral metastatic tumor model preparation

The experimental rabbits underwent a standard 7-day acclimatization period and were closely monitored for any behavioral abnormalities. Prior to surgery, all rabbits were prevented from consuming food or water during an 8-h fasting period. Sixty-eight large New Zealand White rabbits were selected for weight measurement. Anesthesia was induced using 3% pentobarbital (1 mL/kg) administered intravenously at the margin of the ear; then, the rabbits were securely immobilized on a custom-made plate. The targeted puncture area was pre-stripped of hair, and the erector spinae muscle, positioned 5 mm from the central edge of the lumbar two vertebrae, was identified as the seeding point for the tumor. The puncture path and direction were meticulously planned through CT scanning. Following skin disinfection around the puncture site, a 19-gauge puncture needle was employed to traverse the predetermined path. Once the CT scan confirmed the needle tip's precise position at the target point, the core was withdrawn, and two small pieces of carefully selected VX2 tumor tissue were inserted. Gelatin sponge strips were used to seal the needle path. The puncture needle was swiftly withdrawn, and pressure was applied to the puncture site for 2 min. Routine postoperative sterilization was carried out for three consecutive days, accompanied by an intramuscular administration of 0.4MU units of penicillin once daily(Fig. 1.).

**Model evaluation** MR scans were conducted every 3 days, starting from the seventh day after tumor implantation, to monitor and confirm successful implantation in experimental rabbits. The study inclusion criteria were as follows:1. The presence of a single focal nodule in the paravertebral region within the size range of 1.5–2.0 cm; 2. Absence of subcutaneous metastasis; 3. No motor deficits or abnormalities in movement; 4. BRPS<sup>7</sup> score of ≥ 5 points. Separately, the exclusion criteria included the following: (1) Tumor diameter of > 2.0 or < 1.5 cm; (2) Presence of multiple metastases of the tumor; (3) Movement disorder or abnormal movement; (4) BRPS score of < 5 points.

Ablation procedures

The ablation techniques employed in this experiment included CA and MWA.

Experimental grouping and preoperative preparation

The success rate of CT-guided modeling for paravertebral metastases was 88.23% (60/68 rabbits). One rabbit failed to be successfully implanted, two rabbits experienced metastasis in other areas, and five rabbits did not meet the inclusion criteria based on pain scores; thus, the remaining 60 rabbits with successfully prepared tumor models were randomly assigned to the CA group (n=30) or the MWA group (n=30). Both CA and MWA procedures were performed by two physicians with intermediate or higher professional titles, each with more than 5 years of experience in ablation surgery. Prior to the ablation surgery, CT scans of the affected vertebrae

MR sequence	Scanning direction	TE (ms)	TR (ms)	Slice thickness (mm)	NEX	FA	FOV (mm)
T1WI Vibe Dixon	Axial	22.0	720	3.0	4	10.0	230×230
Haste T2WI fs	Sagittal	110.0	3000	2.0	4	120.0	260×211
Haste T2WI fs	Axial	98.0	3000	3.0	4	120.0	180×180
DWI	Axial	50.0	3000	3.0	2	90.0	230×230
T1WI Vibe Dixon C+	Axial	5.0	10.0	2.0	4	10.0	260×211

**Table 1.** MR sequences and parameters. *Abbreviations:* MR, magnetic resonance; FA, flip angle; FOV, field of view; NEX, number of excitations; TE, echo time; TR, repetition time.

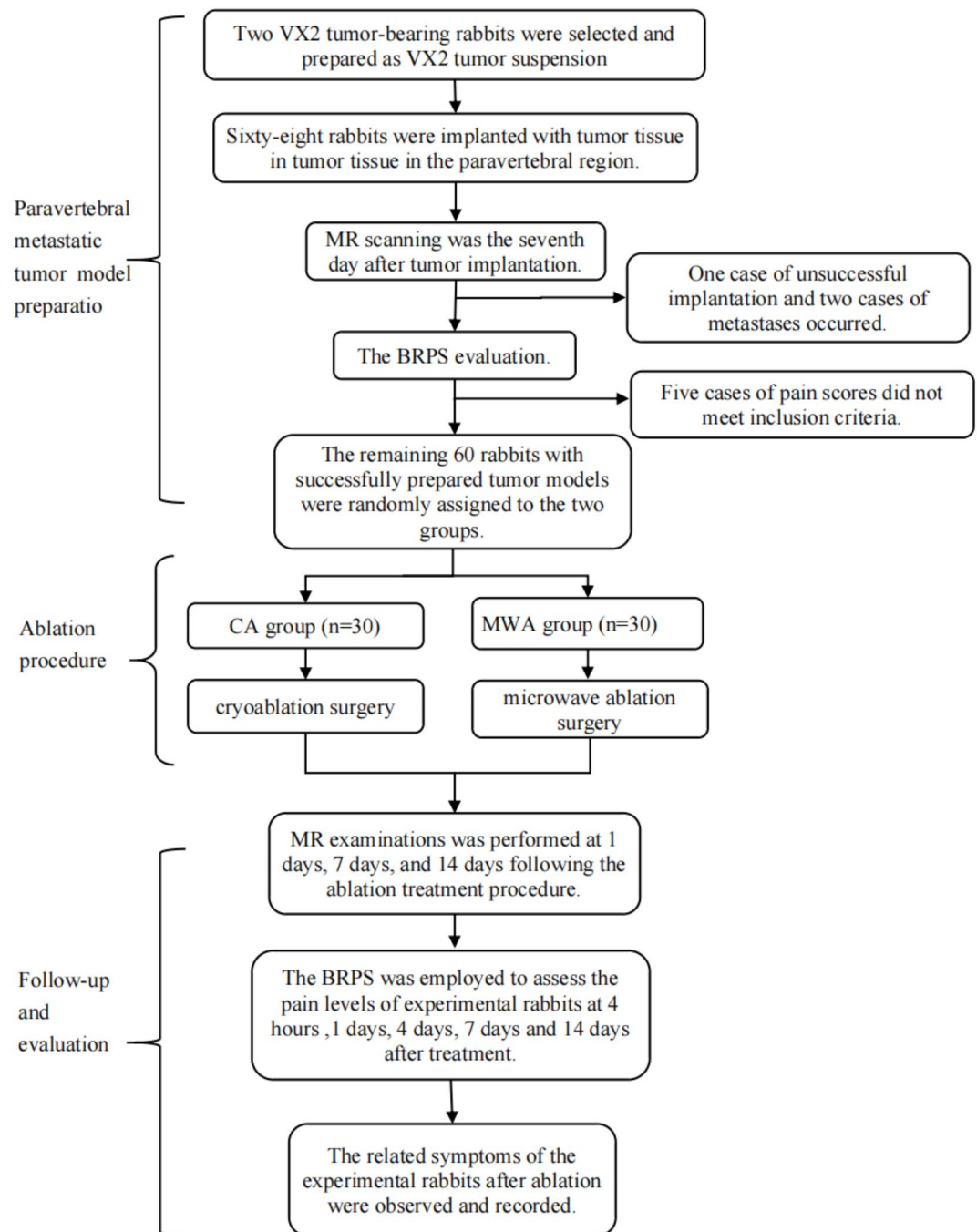


**Fig. 1.** The experimental flow chart.

were taken, and the location and direction of the needle puncture point were determined based on the lesion's location and size, aiming to simulate the extent of the ablation area and minimize the possibility of the dural sac not being covered by the ablation area.

### CA procedure

Following the proposed puncture path identified through CT scanning, a 17-gauge CA needle (Targeted Knife; Shanghai Orientation Medical Co., Ltd.) was progressively advanced to the target area under CT guidance. The tip of the CA needle extended beyond the tumor edge by 0.5 cm. A double-cycle CA mode (freezing–rewarming–freezing) was adopted, and the CT scans were monitored every 3 min to ensure that the iceballs covered the entire tumor (Fig. 2 C). If the edge of the iceball reached the edge of the dural sac, the CA power was reduced. The CA time was 6–12 min based on tumor size, with the success criterion being complete coverage of the lesion by the ice ball. The rewarming time was 3 min, with a temperature of 40 °C. The ablation time and temperature were recorded. Then, following the completion of the ablation, the needle was withdrawn, and pressure was applied

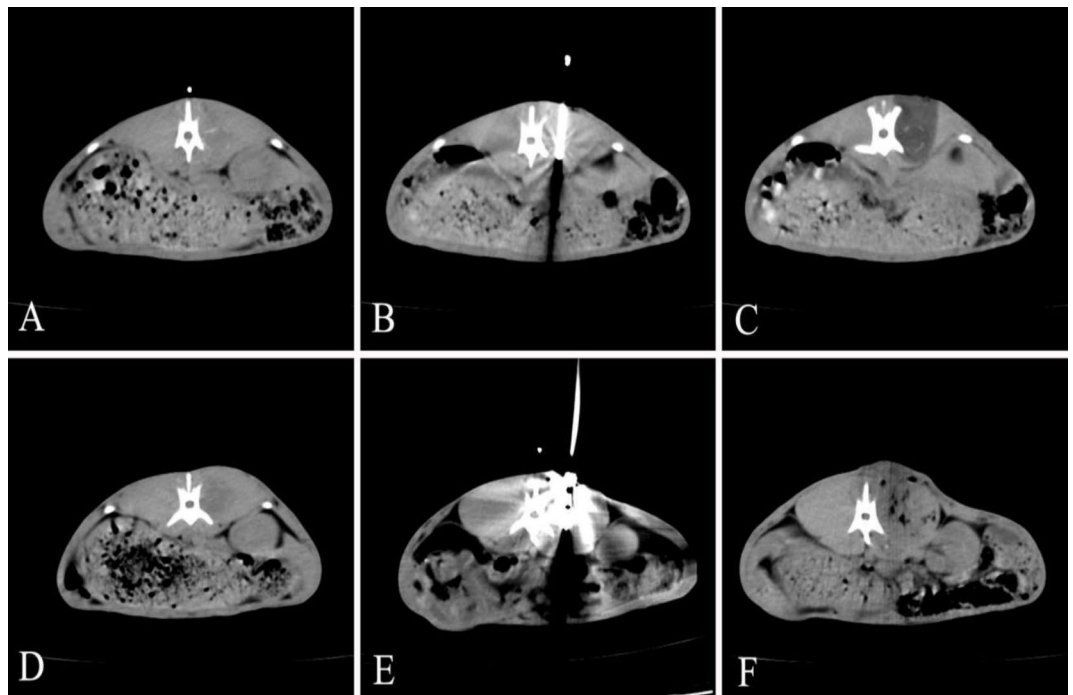


**Fig. 2.** The CT-guided two-group ablation technique. Pre-ablation axial CT images show the right paravertebral tumor of the lesion (**A** and **D**). A CT image taken during the CA procedure shows high-density CA needle penetration into the lesion (**B**). A CT image taken after the CA procedure shows iceball formation completely covering the lesion adjacent to the dural sac (**C**). A CT image taken during the MWA procedure shows high-density MWA needle penetration into the lesion (**E**). A CT image taken after the MWA procedure shows characterized by tumor hypodensity (**F**) and visible bubble formation. CT, computer tomography; CA, cryoablation; MWA, microwave ablation.

to the puncture point for about 2 min. Immediate post-procedure CT imaging and a thorough examination were completed to reveal complications like bleeding, skin damage, and lower-limb sensory impairment. After confirming the absence of any abnormalities, the rabbits were returned to the animal experiment center. As a preventive measure against infection, all experimental rabbits received intramuscular injections of penicillin (400,000 U/day) for three consecutive days (Fig. 2).

#### *MWA procedure*

The MWA procedure was conducted under CT guidance, with the ablation needle progressively advancing along the predetermined path, penetrating the tumor. Based on pre-experiment data, ablation power ranging from 25 to 35 W with an application duration of 4–6 min was adopted, with adjustments made according to the location and size of the tumors. The operators ensured that the ablation area adequately covered the tumor while minimizing damage to adjacent structures, such as the dural sac. This approach enhanced both the safety and efficacy of the optimized procedure. Throughout the ablation process, the position of the ablation needle and the ablation power were dynamically adjusted based on the tumor's size and shape. The ablation area was also modified to ensure comprehensive coverage of the tumor while minimizing the involvement of the dural sac in the ablation region. Following needle withdrawal, CT imaging, and a physical examination were again promptly conducted to reveal complications like bleeding, skin damage, and sensory disorders in the lower limbs. Corresponding data were recorded and conveyed to the animal experimental center. As a standard postoperative procedure to prevent infection, intramuscular injections of penicillin were routinely administered (Fig. 2.).

#### **Follow-up and observation indicators**

All experimental rabbits underwent MR examinations at 1, 7, and 14 days following the ablation treatment procedure. The assessment of ablation effectiveness was conducted by two attending radiologists using a combination of imaging examination results and the Response Evaluation Criteria in Solid Tumor (RECIST)<sup>8</sup>. The criteria for evaluating complete ablation included: no enhancement was observed in the arterial phase at the location of the original lesion or at the edge of the ablation area, the regular annular enhancement area in the venous phase completely covers the original lesion. Additionally, diffusion-weighted imaging (DWI) revealed no diffusion limitation, and no tumor activity was detected in the scan. Complete ablation was confirmed when no enhancement nodule in the arterial phase at the location of the original lesion or the edge of the ablation area could be found and when there was no diffusion limitation on DWI, with the scan indicating an inactive tumor. If arterial phase-enhancing nodules or nodules with restricted diffusion on DWI are observed at the original lesion site or at the edge of the ablation zone, they are considered residual ablation tumors.

- The BRPS was used to evaluate the pain levels of rabbits both before and after ablation procedure. Benato et al.<sup>7,9</sup> Previously demonstrated that BRPS is a clinically valid and reliable tool for quantifying pain in rabbits. Rabbits with pain scores of  $\geq 5$  points on the BRPS were recommended for analgesic intervention. In this experiment, the BRPS was employed to assess the pain levels of experimental rabbits before surgery and at 4 h and 1, 4, 7, and 14 days after treatment, respectively. Total scores ranged from 0–18 points, with 0 points indicating an absence of pain and 18 points signifying severe extreme pain. Higher scores on the scale indicated more pronounced pain was being experienced by the rabbits.
- The procedure time was measured from the time of anesthetic injection to the time of ablation needle removal. The experimental rabbits were followed up until 21 days after ablation. The related symptoms of the experimental rabbits after ablation were observed and recorded, such as the absence of complications such as skin injury, hemorrhage, needle tract metastasis, and lower-limb sensory impairment.

### Statistical analysis

- Statistical analysis of the data was conducted using Statistical Package for Social Sciences software (version 26.0, IBM Corp.) software. Numerical data were presented as the number and percentage (%) of cases for categorical variables. For continuous variables, such as tumor size and procedural time, an independent-samples t-test was conducted to compare the means between the two treatment groups (CA and MWA). To compare the complete ablation rate and complication rate between the two groups, a chi-squared test ( $\chi^2$  test) was performed. To assess the changes in pain scores within each group, a paired-samples t-test was used to compare the preoperative and postoperative pain scores measured by the BRPS. Statistical significance was considered at  $P < 0.05$ , and a highly significant difference was denoted at  $P < 0.001$ .

### Statement

The rabbits used in the experiments were sourced from the Experimental Animal Center of North Sichuan Medical College (License no. SYXK (Sichuan) 2008-076), and their care, feeding, and management strictly adhere to the regulations set forth by the Experimental Animal Center of North Sichuan Medical College. The Animal Ethics Committee of North Sichuan Medical College granted approval for the experimental study (approval no. NSMC Ethical Animal Review (2023)067). This study is in accordance with ARRIVE guidelines. All experiments conducted in this study were in strict accordance with relevant guidelines and regulations.

## Results

### Comparison of complete ablation rate and operation time

All ablation procedures were successful, achieving a 100% technical success rate with 60 tumor-bearing rabbits successfully ablated. The surgical time in the CA group was longer ( $42.6 \pm 2.34$  min) compared to the MWA group ( $28.2 \pm 3.35$  min), and the difference in ablation procedure time between the two groups was statistically significant ( $P < 0.001$ ) (Table 2).

- Before treatment, there was no statistically significant difference in the maximum tumor diameter, tumor area, or the distance from the tumor edge to the dural sac between the two groups ( $P > 0.05$ ). After treatment, 86.67% (26/30) of cases in the CA group and 63.33% (19/30) in the MWA group, were completely ablated, and the difference between these two groups was statistically significant ( $\chi^2 = 4.356$ ,  $P = 0.037$ ) (TabFig. Fig. 3).

### Pain relief

Before treatment, there was no statistically significant difference in BRPS scores for pain between the two groups of experimental rabbits ( $P > 0.05$ ). After treatment, however, a comparative analysis of pain scores at five time points (4 h and 1, 4, 7, and 14 days) between the CA and MWA groups revealed that the pain scores in the CA group were consistently lower than those in the MWA group, and the differences between the two groups were statistically significant ( $P < 0.001$ ).

Comparing the pre-treatment pain scores in the two groups of rabbits, the post-treatment pain scores at 4 h and 1, 4, 7, and 14 days showed a gradual decrease. The differences in pain scores at the five time points after treatment were statistically significant compared to the pre-treatment scores in both groups ( $P < 0.05$ ) (Table 2). This indicates a consistent trend of decreasing pain scores during the observation period.

### Follow-up and complications

The total complication rate was 10.00% (3/30) in the CA group and 33.30% (10/30) in the MWA group, and the difference was statistically significant ( $\chi^2 = 4.812$ ,  $P = 0.028$ ). One case of hemorrhage (1/30, 3.33%) and two cases of skin injury (2/30, 6.67%) were observed in the CA group. Compared to the occurrence of postoperative complications in the CA group, the probability of postoperative complications in the MWA group was greater, and the situation of complications was more serious, with three cases of skin injury (3/30, 10.00%), four cases of lower-limb sensory impairment (4/30, 13.33%), and three cases of death (3/30, 3.33%) occurred (Table 4).

## Discussion

Due to the unique anatomical location of paraspinal metastatic tumors, the ablation treatment process can lead to serious complications, such as spinal cord and nerve injuries. Comparative studies on the short-term efficacy and safety of CA and MWA in treating paraspinal metastatic tumors have been lacking in previous reports. Therefore, this study aimed to evaluate and compare the postoperative pain relief, tumor control, and postoperative complications of CA and MWA for the treatment of pain from paravertebral metastases by establishing a rabbit paravertebral metastasis model.



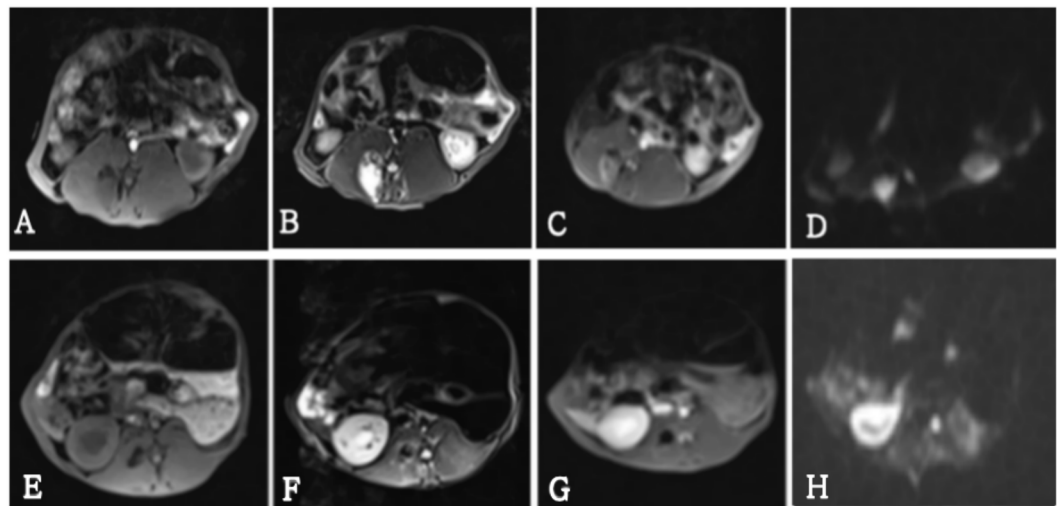


**Fig. 3.** MR image of complete ablation of paravertebral metastasis. (A–D) Preoperative MR images of paravertebral metastasis showing that the lesion was located in the right paravertebral body, with low signal on T1WI (A), high signal on T2WI (B), mild-to-moderate enhancement on enhanced scanning (C), and high signal on DWI (D), respectively. (E–H) MR image after ablation. Postoperative T1WI and T2WI images reveal a decrease in the signal intensity of the lesion compared to preoperative levels (E, F), and the enhanced scanning shows no contrast filling of the lesion after ablation (G). The postoperative DWI showing decreased high signal in the lesion(H).

Outcome	CA(n=3)	MWA(n=30)	p-value
Maximum diameter of tumor (cm)	1.85 ± 0.22	1.80 ± 0.35	0.412
Tumor area (cm <sup>2</sup> )	3.08 ± 0.17	2.96 ± 0.16	0.449
Distance from tumor margin to dural sac (mm)	2.82 ± 0.54	2.77 ± 0.56	0.720
Complete ablation rate (%)	86.67% (26/30)	66.67% (19/30)	0.037
Operation time (min)	42.8 ± 2.64	28.7 ± 3.15	<0.001

**Table 2.** Comparison of the effects of CA and MWA in the treatment of rabbit VX2 paravertebral metastases.

Time point	CA (n = 30)	MWA (n = 30)	t-value	P-value
Before treatment	8.89 ± 0.15	8.93 ± 0.14	−0.794	0.430
4 h after treatment	4.38 ± 0.15*	4.81 ± 0.46*	−4.811	<0.001
1 day after treatment	3.51 ± 0.28*	4.03 ± 0.17*	−9.296	<0.001
4 days after treatment	2.78 ± 0.16*	3.64 ± 0.18*	−19.453	<0.001
7 days after treatment	2.65 ± 0.17*	3.31 ± 0.23*	−12.437	<0.001
14 days after treatment	2.63 ± 0.21*	3.14 ± 0.13*	−11.771	<0.001

**Table 3.** Comparison of the BRPS scores of rabbits in different periods. Note: \* $P < 0.05$  compared to the group before treatment; data are shown as mean ± standard deviation.

Postoperative Complications	CA (n = 30), n (%)	MWA (n = 30), n (%)	P-value
Bleeding	1/30 (3.33%)	0/30 (0.00%)	/
Skin damage	2/30 (6.67%)	3/30 (10.00%)	/
Lower-limb sensory impairment	0/30 (0.00%)	4/30 (13.33%)	/
Death	0/30 (0.00%)	3/30 (10.00%)	/
Total complications	3/30 (10.00%)	10/30 (33.33%)	0.028

**Table 4.** Complications after ablation in two groups.

### Tumor control

The results of this experimental study revealed a complete ablation rate of 91.67% in the CA group and 66.67% in the MWA group, consistent with previous findings on the treatment of paravertebral metastases with MWA<sup>10</sup>. The assessment of ablation margins in MWA can be challenging, relying on a reduction in the density of the ablation zone and the generation of air bubbles. Empirical variations in ablation power and time based on tumor location and surrounding structures can also occur.

In contrast, the iceball formed by CA was clearly observable on CT scan images, allowing for accurate monitoring of the ablation iceball boundary to achieve more precise control of the safe ablation boundary. In CA, when the edge of the iceball reaches the edge of the dural sac, the ablation power can be reduced to acutely maintain the size of the iceball. This approach enhances the ablation effect while reducing the risk of both spinal cord and nerve injury. These findings align with the results reported by Bertolotti et al.<sup>11</sup>.

### Pain relief

This study's results indicate that the postoperative pain scores at 4 h, 1 day, and 4 days after CA and MWA for vertebral metastatic tumors are significantly reduced compared to the preoperative pain scores in each group. This suggests that both ablation methods can rapidly alleviate pain by disrupting local sensory nerves and interrupting pain transmission. Furthermore, at 7 days and 14 days postoperatively, the pain scores show a sustained and gradual decline, indicating that both CA and MWA can effectively and durably control tumor-related pain. Analyzing the mechanisms of pain relief for CA and MWA, several reasons may contribute: Firstly, ablation can directly damage adjacent sensory nerve fibers, blocking pain transmission. Secondly, ablation can reduce the volume of the tumor, alleviating pressure on nerve fibers and consequently reducing pain. Thirdly, ablation can disrupt tumor cells, preventing the production of cell factors related to nerve stimulation and reducing pain sensitivity. These results align with previous studies on the mechanisms of pain relief<sup>6,12</sup>. In comparison to other ablation techniques, the extremely low temperature of CA can be considered an anesthetic, not only reducing pain during surgery but also minimizing post-cooling vascular constriction to reduce swelling caused by CA and decrease the release of pain-inducing substances from damaged tissues<sup>13,14</sup>.

### Postoperative complications

When analyzing the reasons for skin damage observed in both groups in this study, we found that, first, compared to deep-seated lesions, vertebral metastatic tumors requiring treatment are located in relatively shallow positions, and the temperature of the ablation zone can easily spread to the skin surface, causing skin damage. Second, during the ablation process, there was no regular replacement of warm gauze to maintain the skin temperature at the ablation site. Therefore, to prevent the temperature of the ablation zone from propagating to the skin surface, it is important to pay attention not only to the physical temperature of the skin but also to the fact that the ablation needle enters the skin site away from the tumor<sup>15</sup>; moreover, improved surgical maneuvering reduces the incidence of skin injuries, consistent with the findings of Auloge et al.<sup>16</sup>. The primary cause of lower-limb sensory impairment following the procedure is likely due to nerve injury and spinal cord injury. This complication can be influenced by several factors, including the technique of ablation, tumor size, and the proximity of the tumor to the spinal cord and nerves. In particular, MWA can cause thermal damage to adjacent neural structures, leading to sensory deficits. In comparison, CA, which offers better visualization of the ice ball during the procedure, may help reduce the risk of such injuries by allowing more precise targeting and minimizing damage to surrounding tissues, including the spinal cord and nerves. These factors should be carefully considered when planning and performing the ablation procedure to reduce the likelihood of postoperative sensory impairment. Postoperative complications play a crucial role in clinical treatment choice; thus, the greater safety of CA makes it more reliable.

### Pros and cons of CA and MWA

While CA's major advantage lies in the ease of monitoring the ablation zone and boundaries, providing more reliable and safer treatment near critical structures, it is a more time-consuming process than MWA. The primary reason is associated with the freeze–thaw cycles and the readjustment and cooling of the cryoprobe in CA treatment. The time for CA procedures is challenging to shorten and optimize, constituting a significant drawback in its clinical application<sup>11,16</sup>. MWA's advantages include generating a larger and hotter ablation zone, along with shorter ablation times. The choice between ablation methods for tumor tissue depends on the tumor's location relative to adjacent structures<sup>17,18</sup>. Furthermore, the dynamic nature of the MWA procedure, which allows for real-time adjustments to both power and needle positioning, provides more precise control over the ablation process. This can help reduce the risk of incomplete ablation and minimize collateral damage. However, despite these precautions, MWA still faces challenges in clearly delineating the ablation zone, which may result in unintentional damage to surrounding tissues and vulnerable structures. To address these issues, future studies could explore the optimal power settings and application durations for different tumor types, refining the technique to further enhance both its efficacy and safety.

### Limitations

There are some limitations to this study. First, the short follow-up period of only 14 days is a notable limitation. A longer follow-up period would be required to assess the long-term oncological outcomes. Second, while the sample size in this study meets statistical requirements, it is still relatively small. In future studies, increasing the sample size would provide more robust data and help improve the generalizability of the results. Third, the assessment of complete ablation after ablative treatment relies solely on imaging results, without dynamic observation of pathological changes, which may introduce some bias. To overcome this limitation, future studies could incorporate histopathological examinations to provide a more accurate

assessment of the ablation zone and its completeness. Fourth, the relationship between MWA output power and the size of the ablation zone was not evaluated in this study. Since we avoided using high output power to ensure the safety of the experimental rabbits, this limited our ability to assess the full range of ablation outcomes. Future studies should explore the optimal power settings for different tumor sizes and investigate how MWA output power influences the size and efficacy of the ablation zone, to better guide clinical practice. Fifth, the study primarily demonstrates the potential safety and pain-relief benefits of cryoablation rather than its oncologic outcomes. Finally, although the rabbit model is widely used in preclinical studies due to its relative similarity to human tumor biology, there are challenges in translating the findings from animal models to human clinical settings.

## Conclusion

This study found that CA was more effective and safer than MWA for treating paravertebral metastases. CA had a higher complete ablation rate, lower post-ablation pain, and fewer complications than MWA. However, CA required longer operation times, which suggests the need for further optimization. Overall, CA may be more beneficial for tumors near critical structures like the spinal cord, due to its better visibility. While MWA could be preferred for smaller tumors or when a quicker procedure is needed. But it is important to note that the oncologic efficacy of both methods cannot be fully assessed within the short timeframe of this study. Further research with larger samples and longer follow-ups is needed to refine treatment protocols.

## Data availability

Raw data obtained and analyzed from this study are available from the corresponding author upon reasonable request.

Received: 28 January 2024; Accepted: 5 March 2025

Published online: 19 March 2025

## References

1. Pretell-Mazzini, J., Younis, M. H. & Subhawong, T. Skeletal muscle metastases from carcinomas: A review of the literature. *JBJS Rev.* **8**, e1900114–1900118 (2020).
2. Sgalambro, F., Zugaro, L. & Bruno, F. Interventional radiology in the management of metastases and bone tumors. *J. Clin. Med.* **11**, 3265 (2022).
3. Li, Y., Guo, Z., Wang, H. T., Yang, X. L. & Liu, C. F. The treatment of paravertebral malignant mesenchymal tumor pain with cryoablation. *Cryobiology* **69**, 169–173 (2014).
4. Zhicheng, Z. H. H. et al. Efficacy analysis of CT-guided 125I seed implantation assisted by 3D printing non-coplanar templates combined with percutaneous vertebroplasty in the treatment of spinal metastases[J]. *Clin. J. Med. Officers.* **49**, 273–275 (2021).
5. Papalexis, N. et al. The new ice age of musculoskeletal intervention: role of percutaneous cryoablation in bone and soft tissue tumors. *Curr. Oncol.* **30**, 6744–6770 (2023).
6. Yao, Y., Zhu, X. & Zhang, N. Microwave ablation versus radiofrequency ablation for treating spinal metastases. *Med. (Baltim).* **102**, e34092 (2023).
7. Benato, L., Murrell, J. & Rooney, N. Determining a cut-off point for intervention analgesia in rabbits using the Bristol rabbit pain scale. *Vet. Rec.* **193**, e2995 (2023).
8. Lei Jing, Z. Z. et al. Evaluation criteria and evaluation progress of imaging efficacy of solid tumors [J]. *Funct. Mol. Med. Imaging(Electronic Edition)*. **4**, 619–625 (2015).
9. Benato, L., Murrell, J. & Rooney, N. Bristol Rabbit Pain Scale (BRPS): clinical utility, validity and reliability. *BMC Vet Res* **18**, 341 (2022).
10. Sagoo, N. S. et al. Microwave ablation as a treatment for spinal metastatic tumors: A systematic review. *World Neurosurg.* **148**, 15–23 (2021).
11. Bertolotti, L. et al. Radiofrequency ablation, cryoablation, and microwave ablation for the treatment of small renal masses: efficacy and complications. *Diagnostics (Basel)*. **20**, 388–391 (2023).
12. Mantyh, P. W., Clohisy, D. R. & Koltzenburg, M. Molecular mechanisms of cancer pain. *Nat. Rev. Cancer.* **2**, 201–209 (2002).
13. Jennings, J. W. et al. Cryoablation for palliation of painful bone metastases: the MOTION multicenter study. *Radiol. Imaging Cancer.* **3**, e200101 (2021).
14. Khanmohammadi, S., Noroozi, A., Yekaninejad, M. S. & Rezaei, N. Cryoablation for the palliation of painful bone metastasis: A systematic review. *Cardiovasc. Intervent Radiol.* **46**, 1469–1482 (2023).
15. Kurup, A. N. et al. Avoiding complications in bone and soft tissue ablation. *Cardiovasc. Intervent Radiol.* **40**, 166–176. <https://doi.org/10.1007/s00270-016-1487-y> (2017).
16. Auloge, P. et al. Percutaneous cryoablation for advanced and refractory extra-abdominal desmoid tumors. *Int. J. Clin. Oncol.* **26**, 1147–1158 (2021).
17. Alhasan, A. S. et al. Complication rates and risk of recurrence after percutaneous radiofrequency ablation and microwave ablation for the treatment of liver tumors: a Meta-analysis. *Acad. Radiol.* **31**, 1288–1301 (2024).
18. Sciubba, D. M., Pennington, Z. & Colman, M. W. Spinal metastases 2021: a review of the current state of the Art and future directions. *Spine J.* **21**, 1414–1429 (2021).

## Acknowledgements

We thank LetPub ([www.letpub.com](http://www.letpub.com)) for its linguistic assistance during the preparation of this manuscript.

## Author contributions

Z-Z.S. and B.L. wrote the main manuscript text, Z-Z.S. and Y-F.Z. prepared Figs. 1, 2 and 3. B.L. carried out bioinformatic analyses and revised the manuscript. Z-Z.S. and B.L. conceived the study and revised the manuscript. All authors reviewed the manuscript.



## Funding

This work was supported by project of Science and technology of Nanchong City (NO. 23JCYJPT0042); Doctoral Startup Fund of the Affiliated Hospital of North Sichuan Medical College: (NO. ZX-51130001-2023-614); The Primary Health Development Research Center of Sichuan Province Program (NO: SWFZ24-Y-46).

## Competing interests

The authors declare no competing interests.

## Additional information

**Correspondence** and requests for materials should be addressed to B.L.

**Reprints and permissions information** is available at [www.nature.com/reprints](http://www.nature.com/reprints).

**Publisher's note** Springer Nature remains neutral with regard to jurisdictional claims in published maps and institutional affiliations.

**Open Access** This article is licensed under a Creative Commons Attribution-NonCommercial-NoDerivatives 4.0 International License, which permits any non-commercial use, sharing, distribution and reproduction in any medium or format, as long as you give appropriate credit to the original author(s) and the source, provide a link to the Creative Commons licence, and indicate if you modified the licensed material. You do not have permission under this licence to share adapted material derived from this article or parts of it. The images or other third party material in this article are included in the article's Creative Commons licence, unless indicated otherwise in a credit line to the material. If material is not included in the article's Creative Commons licence and your intended use is not permitted by statutory regulation or exceeds the permitted use, you will need to obtain permission directly from the copyright holder. To view a copy of this licence, visit <http://creativecommons.org/licenses/by-nc-nd/4.0/>.

© The Author(s) 2025